

# Integrated DLP and DIW 3D printer for flexible electronics

Qinghua Yu<sup>1†</sup>, Zixiao Zhu<sup>1†</sup>, Xiru Fan<sup>1</sup> and Dong Wang<sup>1\*</sup>

<sup>1</sup> State Key Laboratory of Mechanical System and Vibration, School of Mechanical Engineering, Shanghai Jiao Tong University, Shanghai 200240, China, and Meta Robotics Institute, Shanghai Jiao Tong University, Shanghai 200240, China  
wang\_dong@sjtu.edu.cn (D.W.)

*†: These authors contribute equally to this work.*

**Abstract.** 3D printing is an efficient way to fabricate flexible electronics due to its ability to fabricate complex soft structures. However, the development of 3D printing flexible electronics is hindered by the development of multi-material 3D printing system that can integrate digital light processing and direct ink writing printing technologies. In this work, we develop an integrated DLP and DIW 3D printer that can fabricate multimaterial flexible electronics automatically. Complex matrix structures can be fabricated using bottom-up DLP printing, while the conductive electronics can be directly written on the matrix using DIW printing. Flexible electronics strain sensors and a multi-material soft pneumatic actuator are successfully printed. This work paves the way to fabricate flexible electronics automatically.

**Keywords:** Flexible Electronics, 3D Printing, Integrated Fabrication.

## 1 Introduction

Flexible electronics [1, 2] consisting of soft matrix and conductive electronics show promising applications in areas such as stretchable electronics [3, 4], medical monitoring, diagnosis, and treatment [5-7], and soft robotics [8, 9] due to its great flexibility and ductility [10]. As traditional manufacturing methods cannot meet their manufacturing requirements [11, 12], 3D printing [13] have gained increasing attention due to its ability to fabricate complex soft structures [14] and print flexible circuit boards with special functions.

However, 3D printing flexible electronics often requires the combination of multiple additive manufacturing technologies [15], which significantly increases the complexity and costs. The development of 3D printing flexible electronics is hindered by the development of multi-material 3D printing system that can integrate digital light processing and direct ink writing printing technologies.

In this work, we develop an integrated DLP and DIW 3D printer that can fabricate multimaterial flexible electronics automatically. Complex matrix structures can be fabricated using bottom-up DLP printing, while the conductive electronics can be directly

written on the matrix. A flexible electronics with embedded conductive wires and a multi-material soft pneumatic actuator is printed by the integrated printer, showing promising application in soft robotics. This work paves the way to fabricate flexible electronics automatically.

## 2 Equipment setup

### 2.1 DLP

Fig. 1(a) shows the principle of bottom-up DLP 3D printing. We develop a DLP printing system composed of a UV projector (Wintech 4710, including a 405nm UV-light source and a DMD module), a beam splitter, a resin tank with a transparent glass window coated with PDMS membrane, and a linear translation stage. The resolution of the projector is 1920 pixels  $\times$  1080 pixels. Compared to top-down DLP 3D printing, bottom-up DLP 3D printing has the advantage of printing more precise and complex models since it is not affected by liquid level fluctuations and splashes, thus the beam position is more stable, and is exempted from liquid level correction.

### 2.2 DIW

The setup of the DIW 3D printer is described below. We use three stepper motors and three screw slides to control the x, y and z direction motions, respectively. An Arduino microcontroller is used as an electronics platform and the upper computer interface was written in Python.

DIW's ink is transferred to a syringe barrel (Nordson EFD) and extruded by a precision fluid dispenser (Nordson EFD). The signal for extrusion is written in G-code to control the dispenser through an electromagnetic relay. Fig. 1(b) shows the schematic of the developed DIW 3D printer.

### 2.3 Integrated DLP and DIW

Fig. 1(c) shows the structure of the developed integrated printer, and Fig. 1(d) shows the process of integrated 3D printing. As shown in Fig. 1(d), the transition between the DLP and DIW 3D printing is operated by a rotation servo. As a bottom-up DLP 3D printing technology is used, after the DLP 3D printing the printing stage should rotate by 180° to facilitate the DIW 3D printing and vice versa. We add an air knife next to the DIW syringe barrel to blow away the residual resin before DIW printing.

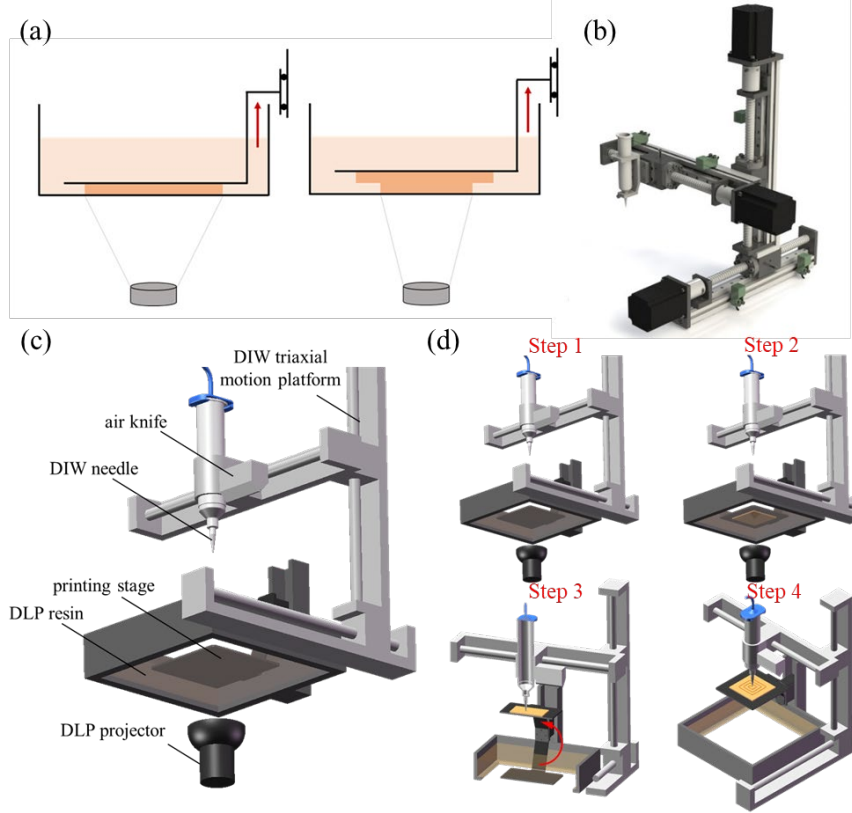


**Fig. 1.** Schematics of the integrated printer. (a) The principle of bottom-up DLP 3D printing. (b) The DIW system. (c) The integrated DLP and DIW 3D printing platform.. (d) Printing process of the integrated printer.

### 3 Printing parameters characterization

#### 3.1 DLP

The hybrid resin (hereinafter referred to as TEEA) is prepared by adding epoxy aliphatic acrylate (EAA) to the commercial UV-curable resin Tango. The weight ratio of Tango and EAA in the TEEA resin is 6:4. Before printing, the CAD model is sliced into images with desired layer thickness.

We measured the light intensity on the focal plane of the DLP projector under different led brightness levels by a UV light irradiation meter (Fig. 2(a)). The maximum irradiation intensity is around  $2700 \mu\text{W}/\text{cm}^2$ .

The resin is cured under UV light irradiation. The accumulated light dose of the resin during a single exposure should be fine-tuned to avoid over-cure and under-cure [16]. If the light intensity is too strong, it will cause over-cure, resulting in warping or edge

curling of the printed piece. When the light intensity is too weak, under-cure will occur and the printed part may fall into the tank causing printing failure.

Through experiments, we determined the optimal combination of printing parameters as 0.1mm per layer at 80% light intensity, with an illumination time of 10s for the bottom layer and 5s for the upper layers. To ensure the adhesion between the printed piece and the printing platform, 10 layers of substrate need to be printed.

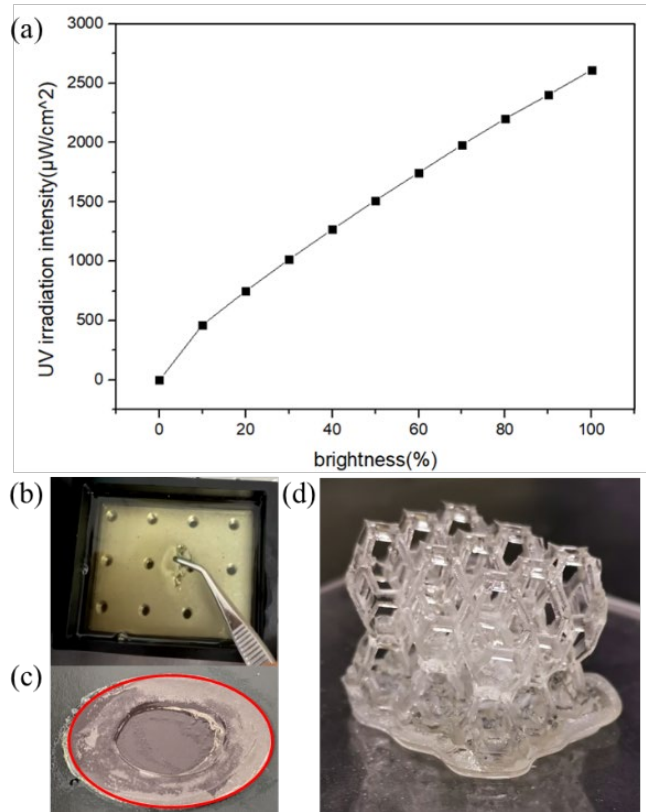


**Fig. 2.** (a) Dependence of the UV irradiation intensity on led brightness level. (b)The printed entity falls into the liquid tank when under-cure occurred. (c) Printing entity shape escapes when over-cure occurred. (d) Printed structure with high precision.

### 3.2 DIW

The key printing parameters in DIW 3D printing are the applied pressure and moving velocity [17]. First, we test a material which is a mixture of 24 wt % Ecoflex 00-30 (Smooth-on inc.) part A/B, 12 wt % SE1700 (Dow Corning Corp.), 1.2 wt % SE1700 curing agent and 62.8 wt % conductive  $\text{Fe}_3\text{O}_4$  powder. The part A/B were prepared in equal mass. Straight lines are printed with different combinations of applied pressure

and the moving velocities of the needle, as shown in Fig 3(a). 300 and 250 kPa pressure is applied, while the moving velocities of the needle vary from 500 to 800 mm/min, with an interval of 100. We can observe that under higher pressure and lower moving velocity, the extruded ink is more curved, which validates that those two parameters have a vital influence on the fabrication quality.

The optimal combination of the applied pressure and the moving velocity of the needle is 160kPa and 600mm/min. Fig. 3(b) shows that DIW ink is extruded into straight lines with the optimal combination of parameters, which facilitates as-design structures fabrication and is necessary for integrated printing.

Then we tested another material which is a mixture of 60 wt % Ecoflex 00-30 part A/B, 30 wt % SE1700 (Dow Corning Corp.), 3 wt % SE1700 curing agent, 5 wt % fumed silica nano and 2 wt % red pigment. The optimal printing parameters combination, which is defined following the same procedure, is 120kPa and 600mm/min. Fig. 3(c) shows the printed structures. An ‘SJTU’ pattern with 2 layers and geometric structures including a cube with 20 layers, a 4-layer square and a 4-layer circle were printed. These printed structures validate that DIW can print both flat and stereoscopic structures under appropriate parameters.

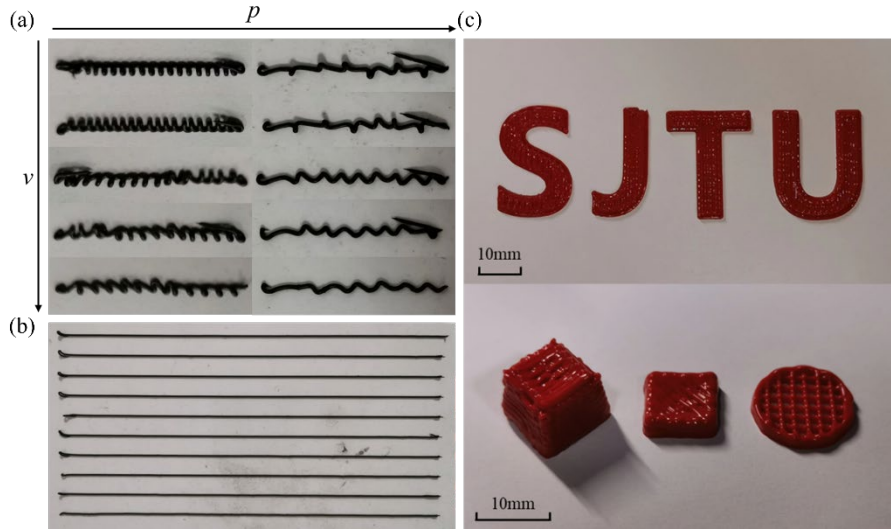


**Fig. 3.** Structures printed by DIW. (a) Straight lines printed with different pressure and velocity. (b) Straight lines printed with appropriate parameters. (c) A 2-layer ‘SJTU’ pattern and geometric structures including a 20-layer cube, a 4-layer square, and a 4-layer circle printed by DIW.

#### 4 Flexible electronics

We then use the DLP and DIW integrated 3D printer to fabricate flexible electronics. The objective structure of the flexible electronics is shown in Fig. 3(a). The conductive wires are embedded inside the soft matrix. Conventional 3D printing method requires the fabrication of half the soft matrix first. The matrix is then peeled away and the

conductive wires are directly written on the matrix, followed by encapsulation using the matrix materials.

Using the DLP and DIW integrated 3D printer, the soft matrix is printed by DLP 3D printing and the conductive wires are written by DIW 3D printing using conductive ink. Thus, the flexible electronics can be fabricated automatically. Fig. 4(b) shows the printed flexible electronics structures with various sizes. Energizing the printed flexible electronics validates the developed integrated 3D printer (Fig. 4(c)).

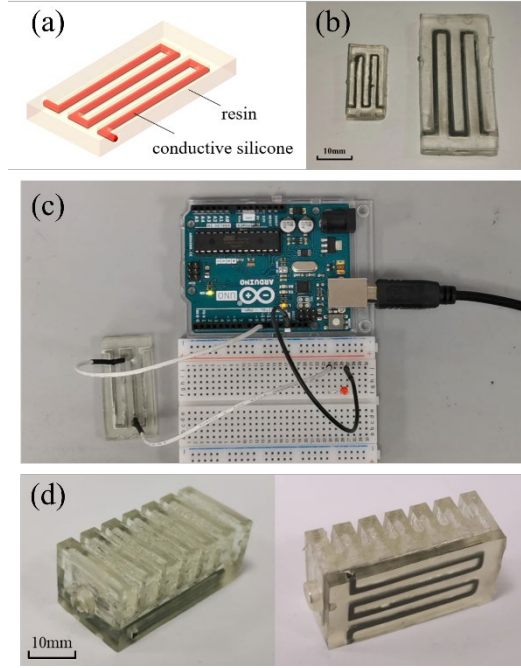


**Fig. 4.** Flexible electronics printed by the integrated 3D printer. (a) The objective structure of flexible electronic devices. (b) Two flexible electronic devices with a size of  $10 \times 20$  and  $20 \times 40$ , respectively. (c) Energized flexible electronic devices. (d) Multimaterial soft pneumatic actuator.

Through testing with the LCR machine, we have validated the sensitivity and reliability of the strain resistance changes in multi-material flexible electronic devices which can serve as strain sensors. This provides strong support and evidence for their application. Further research and development will promote the application and innovation of multi-material flexible strain sensors, bringing more possibilities for future smart materials and flexible electronic devices.

Building on the foundation of multi-material flexible strain sensors, we have fabricated a multimaterial soft pneumatic actuator by incorporating a bendable structure with the multimaterial flexible strain sensor, as shown in Fig. 4(d). When the air chambers are inflated with a syringe, the actuator will bend and the sensor will conduct. Conversely, if the syringe is used to extract air from the air chambers, the actuator will

bend in the opposite direction and the sensor will stretch. This bending and reverse bending mechanism controlled by the air chambers enables multi-material flexible actuators to have controllable deformation characteristics. The strain sensor is capable of measuring tensile strain and bending angle of the actuator by mapping the relation between strain/bending angle and resistance change. This provides broad prospects for their application in fields such as programmable robots, flexible manipulators, and artificial muscles.

## 5 Conclusions

In this work, we develop an integrated DLP and DIW 3D printer that can fabricate multimaterial flexible electronics automatically. Complex matrix structures can be fabricated using bottom-up DLP printing, while the conductive electronics can be directly written on the matrix. Flexible electronics with embedded conductive wires are 3D printed, which show high conductivity, and changing resistance while stretching. The printed multimaterial flexible electronics devices show a promising application as a soft sensor. This work paves the way to fabricate flexible electronics automatically.

## References

1. Peng, X., et al., *Integrating digital light processing with direct ink writing for hybrid 3D printing of functional structures and devices*. Additive Manufacturing, 2021. **40**.
2. Li, Z., et al., *Hydrogel-elastomer-based stretchable strain sensor fabricated by a simple projection lithography method*. International Journal of Smart and Nano Materials, 2021. **12**(3): p. 256-268.
3. Ge, Q., et al., *3D printing of highly stretchable hydrogel with diverse UV curable polymers*. Sci Adv, 2021. **7**(2).
4. González-Henríquez, C.M., M.A. Sarabia-Vallejos, and J. Rodríguez-Hernandez, *Polymers for additive manufacturing and 4D-printing: Materials, methodologies, and biomedical applications*. Progress in Polymer Science, 2019. **94**: p. 57-116.
5. Pettersson, A.B.V., et al., *Main Clinical Use of Additive Manufacturing (Three-Dimensional Printing) in Finland Restricted to the Head and Neck Area in 2016-2017*. Scand J Surg, 2020. **109**(2): p. 166-173.
6. Xu, Y., et al., *In-situ transfer vat photopolymerization for transparent microfluidic device fabrication*. Nat Commun, 2022. **13**(1): p. 918.
7. Zheng, B., et al., *Direct Freeform Laser Fabrication of 3D Conformable Electronics*. Advanced Functional Materials, 2022. **33**(1).
8. Mishra, A.K., et al., *Autonomic perspiration in 3D-printed hydrogel actuators*. Sci Robot, 2020. **5**(38).
9. Truby, R.L., et al., *Fluidic innervation sensorizes structures from a single build material*. Sci Adv, 2022. **8**(32): p. eabq4385.
10. Ge, Q., et al., *3D printing of highly stretchable hydrogel with diverse UV curable polymers*. Science Advances, 2021. **7**(2): p. eaba4261.

11. Yan, J., et al., *Direct-ink writing 3D printed energy storage devices: From material selectivity, design and optimization strategies to diverse applications*. Materials Today, 2022. **54**: p. 110-152.
12. Cheng, M., R. Deivanayagam, and R. Shahbazian-Yassar, *3D Printing of Electrochemical Energy Storage Devices: A Review of Printing Techniques and Electrode/Electrolyte Architectures*. Batteries & Supercaps, 2020. **3**(2): p. 130-146.
13. Rayna, T. and L. Striukova, *From rapid prototyping to home fabrication: How 3D printing is changing business model innovation*. Technological Forecasting and Social Change, 2016. **102**: p. 214-224.
14. Urrios, A., et al., *3D-printing of transparent bio-microfluidic devices in PEG-DA*. Lab Chip, 2016. **16**(12): p. 2287-94.
15. Zhang, Y.-F., et al., *Fractal-Based Stretchable Circuits via Electric-Field-Driven Microscale 3D Printing for Localized Heating of Shape Memory Polymers in 4D Printing*. ACS Applied Materials & Interfaces, 2021. **13**(35): p. 41414-41423.
16. Choi, J.W., et al., *Sequential process optimization for a digital light processing system to minimize trial and error*. Sci Rep, 2022. **12**(1): p. 13553.
17. Hmeidat, N.S., et al., *Mechanical anisotropy in polymer composites produced by material extrusion additive manufacturing*. Additive Manufacturing, 2020. **34**.